International Journal of Innovative Computing, Information and Control
Volume **10**, Number **3**, June **2014**

ICIC International ©2014 ISSN 1349-4198
pp. 919-931

RETRIEVAL METHOD BASED ON IPDSH AND R/KPSO

Xu Zhang[1], Baolong Guo[1] and Jengshyang Pan[2]

[1]Institute of Intelligent Control and Image Engineering
Xidian University
No. 2, South Taibai Road, Xi'an 710071, P. R. China
xuzhang@mail.xidian.edu.cn; blguo@xidian.edu.cn

[2]Department of Electronic Engineering
National Kaohsiung University of Applied Sciences
P. O. Box 6079, Station Centre-Ville, Kaohsiung 807, Taiwan
jspan@cc.kuas.edu.tw

Received May 2013; revised October 2013

Abstract. *Considering the fact that the accuracy of the present interest points' detection algorithms usually influenced by the unstable interest points and a wide variety of relevance feedback (RF) algorithms ignore the manifold structure of image's low-level visual features, we presented an improved image retrieval algorithm based on IPDSH (interest point detection combined the feature of SIFT and Harris) and r/KPSO-RF (particle swarm optimization with r- and K-selection for RF). Firstly, we eliminate the unstable interest points in the non-interest regions by IPDSH. Secondly, we calculate the pseudo-Zernike moments and color moment in the local field of the annular region's stable interest points, and then retrieve the image with the weighted feature vector. Thirdly, based on r/KPSO, we define the positive and negative feedback samples as study principle, and optimize weightings according to user's retrieval requirement. Experiments show that the proposed algorithm reduces the impact of unstable interest points and improves the retrieval precision.*

Keywords: Image retrieval, Interest points, R/KPSO, Relevance feedback

1. **Introduction.** At present, image retrieval is an attractive research subject in the multimedia information processing. Meantime, content based image retrieval (CBIR) becomes to solve the problem that the amount of images is too large to retrieve. CBIR aims to analyze the visual content description and features, such as color, texture and shape, for indexing, thereby dispensing keyword assignment work and implementing a more flexible search style [1].

Nevertheless, the existing of semantic gap [2] makes retrieval systems easily misunderstand user's request, which may lead to poor performance. To satisfy various search preferences of the users, many algorithms arise, such as feature extraction algorithms based on interest points and algorithms based on relevance feedback (RF). Zhang et al. proposed a biased maximum margin analysis (BMMA) and a semi-supervised BMMA (SemiBMMA) for integrating the distinct properties of feedbacks and utilizing the information of unlabeled samples for SVM-based RF schemes [3]. Li et al. proposed a query difficulty guided image retrieval system, which can predict the queries' ranking performance in terms of their difficulties and adaptively apply ranking optimization approaches [4]. Chen et al. proposed a multi-points diverse density (MPDD), which were applied to image retrieval and utilized to contain more information. Experiment results show that the performance of MPDD is superior to classical diverse density learning algorithms [5]. Ma et al. proposed an improved RF system based on hybrid PSO and active learning SVM

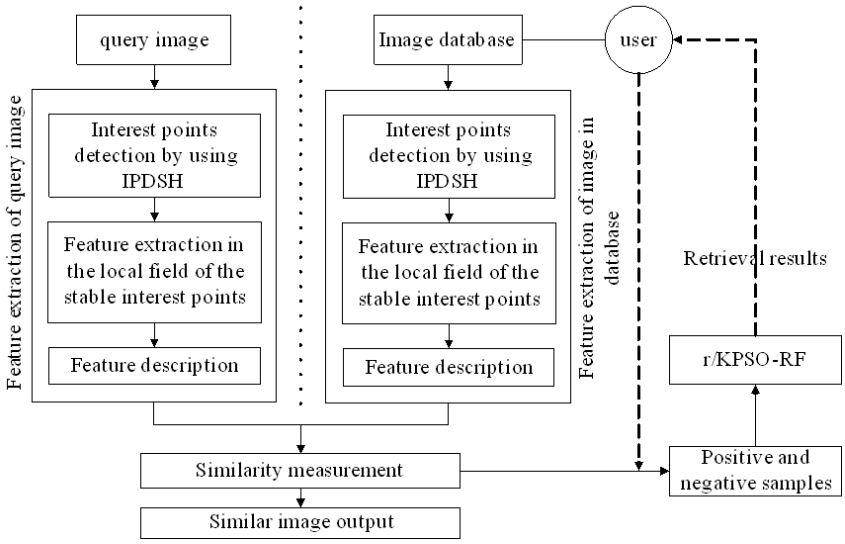

FIGURE 1. Image retrieval structure

model, in which the PSO with/without feature selection can optimalize the parameters and sub-features in the SVM classifier [6].

Although many algorithms promote the retrieval performance, some problems still exist: (1) interest points' detection algorithms is usually influenced by the unstable interest points in the non-interest regions; (2) user interaction is time consuming and tiring, and it is desirable to reduce the number of iterations to convergence; (3) initial result will strongly influence users' feedback and their cognizance of image set, which will cause limitation to the feedback effect; (4) when the size of database increases, the search process converges to a very suboptimal local solution and unable to further explore the image space. Aiming these problems, we apply IPDSH and r/KPSO algorithm to improve the retrieval accuracy. Figure 1 shows the image retrieval structure.

2. **IPDSH Points' Detection.** It is difficult to find a stable and consistent interest point automatically, which are usually defined as corners. There are some popular corner detection algorithms such as Moravec, SUSAN and Harris. Among them, Harris is a most effective method but sensitive to scales, so that precision of corner extraction is completely dependent on the threshold when the response functions implement the non maxima suppression and identify the local maxima. The magnitude of threshold determines the accuracy of detection: corner information will lose if the threshold is too bigger, and false corner will emerge if the threshold is too smaller [7]. Aiming at these problems, a detection method named IPDSH was proposed, which can improve the speed and accuracy of interest points detection. The detailed procedures are as follows.

Convolute the input image $f(x, y)$ with the two-dimensional Gaussian kernel, we can get the multi-scale spaces:

$$S(x, y, \sigma) = G(x, y, \sigma) * f(x, y) \tag{1}$$

The two-dimensional Gaussian kernel is defined as:

$$G(x, y, \sigma) = \frac{1}{2\pi\sigma^2} e^{-(x^2+y^2)/2\sigma^2} \tag{2}$$

Convolution $f(x, y)$ with Difference of Gaussian function (DoG) and obtain the maxima of multi-scale spaces. Suppose that the multi-scale spaces are S, pixel's location of $f(x, y)$

are (x, y), we can define DoG function as:

$$D(x, y, \sigma) = (G(x, y, k\sigma) - G(x, y, \sigma)) * f(x, y) = S(x, y, k\sigma) - S(x, y, \sigma) \quad (3)$$

In which, as a constant, k is usually set to $\sqrt{2}$, $*$ represents the convolutions in x and y directions, and σ is the variance of Gaussian distribution. Then we can define scale spaces' autocorrelation matrix as:

$$A(x, y, \delta_i, \delta_d) = \delta_d^2 G(\delta_i) * \begin{bmatrix} f_x^2(x, \delta_d) & f_x f_y(x, \delta_d) \\ f_x f_y(x, \delta_d) & f_y^2(x, \delta_d) \end{bmatrix} = \begin{bmatrix} \hat{f}_x^2 & \hat{f_x f_y} \\ \hat{f_x f_y} & \hat{f}_y^2 \end{bmatrix} \quad (4)$$

δ_i and δ_d represent the integral and differential scales respectively. $\hat{f}$ is Gaussian filtering of f. Suppose that the eigenvalues of A are λ_1 and λ_2, which represent the principal curvature of autocorrelation function, the calculation formula of different scale spaces are defined as follows:

$$C(x, y, \delta_i, \delta_d) = \det(A(x, y, \delta_i, \delta_d)) - \alpha \cdot trace^2(A(x, y, \delta_i, \delta_d)) = \lambda_1 \cdot \lambda_2 - \alpha \cdot (\lambda_1 + \lambda_2) \quad (5)$$

If the local maxima of C's coordinate falls on the extreme points' neighborhood in the multi-scale spaces, we should retain this extreme point. Otherwise, we should reject this extreme point. Finally, the retentive extreme points are regarded as IPDSH interest points.

Usually, α is a constant (value's range set from 0.04 to 0.06). The calculation method of C's local maxima is according to the magnitude of λ_1 and λ_2. Through the judgment whether Harris corners exist in the local field of extreme points, the unstable interest points will be reduced. This helps to decrease the number of interest points and enhances the significance of interest points' set, so as to improve the precision of retrieval.

We use a test images set (size: 512×512, grayscale: 256-level, as shown in Figure 2) to evaluate the performance of the proposed IPDSH algorithm by comparing with SIFT algorithm. The corresponding detection results are given in Figure 3, where it is found that the total number of interest points detected by IPDSH is lower than by SIFT. The reason is that some unstable interest points are removed.

3. **Feature Extraction.** Transforming the input image data into the set of features is called feature extraction, which is the key technique in CBIR, partly determines the retrieval precision of images. If the features extracted are carefully chosen, it is expected that the features set will extract the relevant information from the input image data. We introduce a weighted feature extraction algorithm combined with annular color moment and pseudo-Zernike moments in order to perform the desired task using this reduced representation instead of the full size input.

(a) Lena (b) Peppers (c) Baboon (d) Barbara

FIGURE 2. Test images dataset

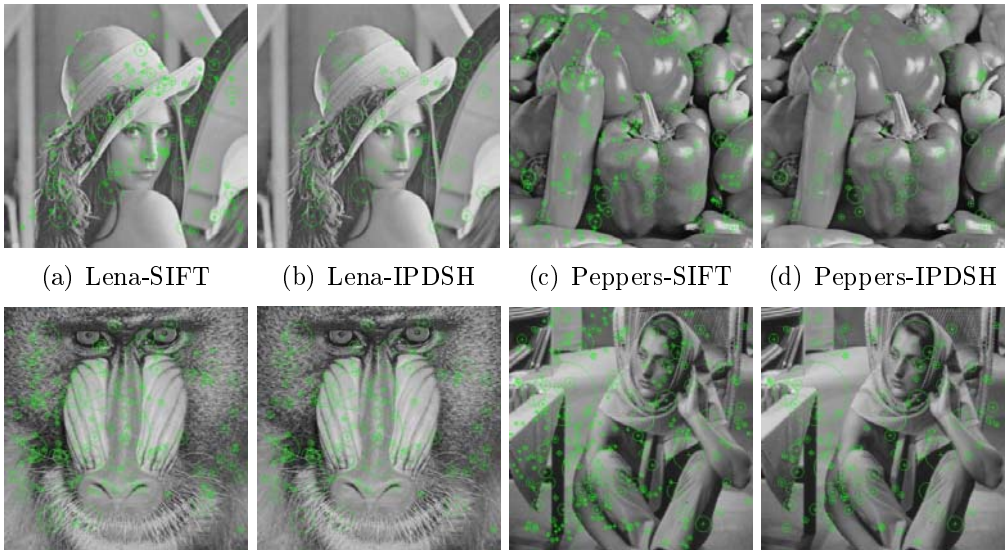

(a) Lena-SIFT (b) Lena-IPDSH (c) Peppers-SIFT (d) Peppers-IPDSH

(e) Baboon-SIFT (f) Baboon-IPDSH (g) Barbara-SIFT (h) Barbara-IPDSH

FIGURE 3. Interest points detection results on test image set: (a) (c) (e) (g) use SIFT algorithm, (b) (d) (f) (g) use IPDSH algorithm

3.1. **Annular color moment.** According to the distribution of interest points, annular division is easy to obtain. Then, we can calculate the annular color histogram, which takes not only the local color feature into consideration but also the space distribution information. With robustness to rotation and translation, the algorithm avoids the shortcoming of losing the location information in color histogram. The detailed procedures are as follows.

Find the centroid M of interest points according to Equation (6):

$$M = (\overline{x}, \overline{y}), \quad \overline{x} = (1/|H|) \sum_{(x,y)\in H} x, \quad \overline{y} = (1/|H|) \sum_{(x,y)\in H} y \tag{6}$$

Calculate the maximum radius R with Equation (7):

$$R = \max_{(x,y)\in H} \left[(x-\overline{x})^2 + (y-\overline{y})^2\right]^{1/2} \tag{7}$$

$$W^k = \left\{(x,y) \middle| \frac{(k-1)R}{N} \le \left[(x-\overline{x})^2 + (y-\overline{y})^2\right]^{1/2} < \frac{kR}{N}, (x,y) \in H\right\} \tag{8}$$

Divide the interest point's area into N annular parts using Equation (8), where N is a natural number. Green '+' represents the centroid, as shown in Figure 4. Each annual's radium is kR/N $(1 \le k \le N)$.

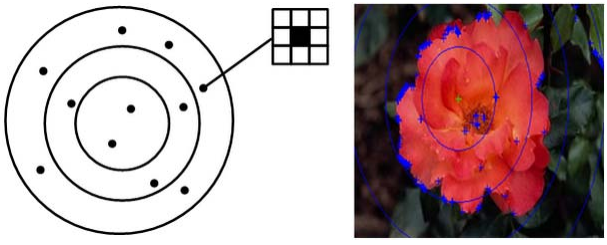

FIGURE 4. Schematic diagram to annular division

Calculate the first-moment $\mu(i,j)$, secondary-moment $\sigma(i,j)$ and third-moment $s(i,j)$ of each interest point's $a \times a$ neighborhood using the following Equation (9), where (i,j) represents the location of interest point, $I_{x,y}$ represents color value of pixel (x,y).

$$\begin{aligned} \mu(i,j) &= \frac{1}{a \times a} \sum_{(x,y) \in a \times a} I_{x,y}, \\ \sigma(i,j) &= \left(\frac{1}{a \times a} \sum_{(x,y) \in a \times a} \left(I_{x,y} - \mu(i,j) \right)^2 \right)^{1/2}, \\ S(i,j) &= \left(\frac{1}{a \times a} \sum_{(x,y) \in a \times a} \left(I_{x,y} - \mu(i,j) \right)^3 \right)^{1/3} \end{aligned} \tag{9}$$

In HSV color space, h, s and v represent the three components of color: hue, saturation and value respectively. Put them into Equation (9), we can obtain 9 color feature components: $\mu_h(i,j)$, $\mu_s(i,j)$, $\mu_v(i,j)$, $\sigma_h(i,j)$, $\sigma_s(i,j)$, $\sigma_v(i,j)$, $S_h(i,j)$, $S_s(i,j)$, $S_v(i,j)$. Then, the linear combination CM^k of nine components represent the annular color moment in k-th annular, as shown in Equation (10), where $k = 1 \cdots N$, w_h, w_s and w_v are constants weight. According to the human vision principle, we usually set $w_h = 0.5$, $w_s = 0.25$, $w_v = 0.25$.

$$\begin{aligned} CM^k = & w_h \left(\sum_{(i,j) \in W^k} \mu_h(i,j) + \sum_{(i,j) \in W^k} \sigma_h(i,j) + \sum_{(i,j) \in W^k} S_h(i,j) \right) \\ & + w_s \left(\sum_{(i,j) \in W^k} \mu_s(i,j) + \sum_{(i,j) \in W^k} \sigma_s(i,j) + \sum_{(i,j) \in W^k} S_s(i,j) \right) \\ & + w_v \left(\sum_{(i,j) \in W^k} \mu_v(i,j) + \sum_{(i,j) \in W^k} \sigma_v(i,j) + \sum_{(i,j) \in W^k} S_v(i,j) \right) \end{aligned} \tag{10}$$

3.2. **Pseudo-Zernike moments.** Pseudo-Zernike [8], which is a kind of invariants moment, is obtained from a group of basic functions $\{V_{nm}(x,y), x^2 + y^2 \leq 1\}$, and performed better than Zernike moment in anti-noise. Using pseudo-Zernike moment based on IPDSH, we obtain a weighting vector with higher accuracy. $V_{nm}(x,y)$ is defined as Equation (11), which is satisfied to Equation (12).

$$\begin{aligned} V_{nm}(x,y) &= V_{nm}(\rho,\theta) = R_{nm}(\rho) \exp(jm\theta) \\ R_{nm}(\rho) &= \sum_{s=0}^{n-|m|} \frac{(-1)^s (2n+1-s)! \rho^{n-s}}{s!(n+|m|+1-s)!(n-|m|-s)!} \end{aligned} \tag{11}$$

$$\begin{aligned} & \iint_{x^2+y^2 \leq 1} V_{nm}^*(x,y) V_{pq}(x,y) dxdy = \frac{\pi}{n+1} \sigma_{np} \sigma_{mq}, \\ & \sigma_{np} = \begin{cases} 1 & n = p \\ 0 & n \neq p \end{cases}, \quad \sigma_{mq} = \begin{cases} 1 & m = q \\ 0 & m \neq q \end{cases} \end{aligned} \tag{12}$$

where, n represents the nonnegative integer, m is the integer ($|m| \leq n$), ρ is radium and θ is the angle of polar coordinates pixels. We defined the $f(x, y)$'s (n, m) step pseudo-Zernike Moments as following equation:

$$\begin{aligned} P_{nm} &= \frac{n+1}{\pi} \iint\limits_{x^2+y^2 \leq 1} f(x,y) V_{nm}^*(x,y) dxdy = \frac{n+1}{\pi} \sum_{\rho \leq 1} \sum_{0 \leq \theta \leq 2\pi} f(\rho,\theta) V_{nm}^*(\rho,\theta) \rho \\ &= \frac{n+1}{\pi} \sum_{\rho \leq 1} \sum_{0 \leq \theta \leq 2\pi} f(\rho,\theta) R_{nm}(\rho) \exp(-jm\theta) \rho \end{aligned} \tag{13}$$

After confirmation of the interest points' location, we can build the origin of polar coordinates, calculate the pseudo-Zernike and convert unit circle to polar coordinates. The pixels out of the polar coordinates will not be calculated.

4. **Similarity Measurement.** Suppose Q represents query image, I represents database image, S_1 represents the similarity of color feature and S_2 represents the similarity of pseudo-Zernike moments in stable interest points' neighborhood, we can define similarity as Equation (14):

$$\begin{cases} S(Q,I) = kcS_1(Q,I) + kpS_2(Q,I), \quad kc + kp = 1 \\ S_1(Q,I) = \sum\limits_{k=1}^{N} \frac{\omega_k}{N} \min(H_k(Q), H_k(I)), \quad S_2(Q,I) = \exp\left\{ - \sum\limits_{k=1}^{N} \frac{\omega_k}{N} [R(Q) - R(I)]^2 \right\} \end{cases} \tag{14}$$

where, kc and kp represent weight values, N represents the number of interest points, ω_k represents the number of interest points in the k-th circle, H represents the calculate equation of color histogram, and R represents the interest points distribution dispersion.

5. **RF Algorithm Based on r/KPSO.** Dohzhansky [9] proposed that most mortality is more directed, generally favoring those individuals with better competitive abilities in the relatively constant tropics. By putting more energy into each offspring and producing fewer total offspring, overall individual fitness is increased. MacArthus and Wilson [10] coined the terms K-selection and r-selection for these two kinds of selections (K refers to carrying capacity and r to the maximal intrinsic rate of natural increase). It is clear that there are two opposing kinds of selections, which usually have to be compromised. Certainly, no organism is completely "r-selected" or completely "K-selected", but all must reach some compromise between the two extremes [11].

We can characterize the r-selection and K-selection as:

r-selection: large number of young; little parental care; a large reproductive effort; productivity; quantitative.

K-selection: small number of young; parental care; a smaller reproductive effort; efficiency; qualitative.

Most characters listed above will be represented to some extent in particles swarm optimization inspired by r- and K-selection (r/K-PSO).

5.1. **r/KPSO.** As a member of swarm intelligence, r/KPSO provides new ideas to solve difficult problems of traditional optimization methods. In r/KPSO, particles update their own speed and position with r-selection and K-selection. Generally, K-selection is applied for those good particles with higher fitness while r-selection for those particles in relatively lower fitness. The advantage of r-selection is that a large number of filial particles can be produced to search potential solution of the optimization problem. The particles

performed K-selection are mainly used to keep the best solution. Let n denote the iteration number, the swarm can be manipulated according to Equation (15):

$$\begin{aligned} v_{id}^{n+1} &= \omega v_{id}^{n} + c_1 r_1 (p_{id}^{n} - x_{id}^{n}) + c_2 r_2 (p_{gd}^{n} - x_{id}^{n}) \\ x_{id}^{n+1} &= x_{id}^{n} + v_{id}^{n+1} \end{aligned} \tag{15}$$

where, $d = 1, 2, \ldots, D$, $i = 1, 2, \ldots, N$, $n = 1, 2, \ldots, G$, G is the iteration number, c_1 and c_2 are positive constants called study factor, r_1 and r_2 are random numbers within the range $[0, 1]$ and ω is the inertia weight. Suppose X_i is the i^{th} particle of the swarm, the swarm with N particles can be thought as the set of particles, as shown in Equation (16):

$$S = \{X_i | i = 1, 2, \ldots, N\}_N \tag{16}$$

Inspired by r-selection and K-selection, the swarm is divided into two sub swarms: r-subswarm whose particles are called r-particles and K-subswam whose particles are called K-particles. In evolution, r-subswarm favors r-selection and K-subswam favors K-selection. Let f represent the fitness function, N fitness function values $f_k(X_i)$, $k \in [1, N]$ can be sorted by ascending order, where k can be thought as the index, as shown in Equation (17).

$$F = \{(f_1, f_2, \ldots, f_N) | f_1 \leq \ldots \leq f_k \leq \ldots \leq f_N\} \tag{17}$$

Let the operator $IND(\cdot)$ present the operation of finding the index of certain particle, we can obtain Equation (18):

$$IND(X_i) = k, \quad iff(X_i) = f_k \tag{18}$$

Then, the total particles N can be ranked and indexed by their fitness values according to Equations (17) and (18). Suppose $L_{\max}$ is the maximum number of r-particles, $rand()$ is a uniformly distributed random number in the interval $[0, 1]$, and $\lceil \cdot \rceil$ rounds the value upward. The number of K-particles H can be described as Equation (19), which represents the high fitness.

$$H = N - \lceil L_{\max} \times rand() \rceil \tag{19}$$

With top H particles of high fitness, the K-subswarm S_K can be described as Equation (20):

$$S_K = \{X_i | X_i \in S, IND(X_i) \geq N - H + 1\}_H \tag{20}$$

Suppose the number of r-particles is L, the r-subswarm is composed of L particles, which is in relatively low fitness, can be presented by Equation (21):

$$S_r = \{X_i | X_i \in S, IND(X_i) \leq N - H\}_L \tag{21}$$

Among the total N particles of the swarm, only top H particles in high fitness can be parted into the K-subswarm and other L particles should lie in r-subswarm. K-selection leads to efficiency and high quality, so in evolution the filial particles should inherit good aspects of the parents. The velocity, the change of particle position, should be limited in a small range. And as a result, ω, c_1 and c_2 in Equation (15) can be in relatively small values. Small velocity means keeping close to the parent and also can be thought to obtain more parent care in K-selection. Every particle in K-subswarm breeds a few progenies. Besides, the optimal strategy of r-selection is to produce progenies as many as possible and takes little care of each individual offspring, so the position of produced particles may vary within a quite large range. ω, c_1 and c_2 also can be in relatively large values.

In K-selection, all progenies generated by K-particles are kept and the progenies become parents in the next epoch. Suppose ρ_k represents the growth rate, the number of K-particles' progenies H_g can be calculated by Equation (22) and the number of progenies

produced L_g can be determined by the growth rate ρ_r, as shown in Equation (23):

$$H_g = \rho_k \times H \tag{22}$$

$$L_g = \rho_r \times L, \quad \rho_r \gg 1 \tag{23}$$

If $L_g + H_g > N$, the swarm size will grow up with exponential rate until some restrictive principles are taken . In general, the K-subswarm size keep fixed if $\rho_k = 1$, so the increase mainly due to the r-subswarm. To keep the swarm size constant, intra-specific competition should be adopted to the r-subswarm. In every evolutionary epoch, only L progenies in top high fitness of the L_g ones can survive in the competition and become parent of the next epoch. A simplified state transition diagram of r/KPSO was shown as Figure 5.

K-swarm produce K-progenies with size H and r-subswarm breed r-progenies with size $Gr \times L$. The selected top L progenies from r-progenies and H produced by K-subswam, total N progenies, are thought as the whole filial generation, ready for next iteration.

Like r- and K-selection in Ecology, r-subswarm and K-subswarm in r/KPSO can be summarized as follows:

r-subswarm: large number of progenies ($\rho_r \gg 1$); velocity in large range (large c_1 and c_2); exploring search space; potential solutions of great quantity.

K-subswarm: few number of progenies ($\rho_k = 1$); velocity in small range; exploiting search space; optimum solution found.

Table 1 shows an example of swarm configurations. ρ_k is unlimited and the parameters of speed for r-subswarm are bigger than the ones for K-subswarm, which can help r-subswarms search the space as large as possible, increase particles' diversity and guarantee the particles not falling into local minimum.

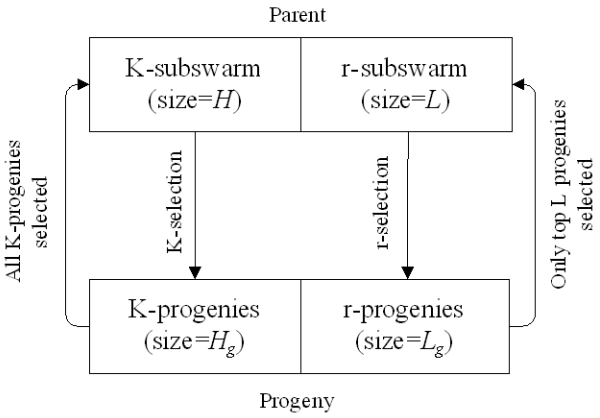

FIGURE 5. Simplified state transition diagram of r/KPSO

TABLE 1. Swarm configurations of r/KPSO implementation

Item	K-subswarm	r-subswarm
G	300	300
Swarm size	H (Equation (19))	$L = 20 - H$
ρ_K	1.0	–
c_1	2.05	2.1
c_2	2.05	3.9
ω	0.6	0.6

Combined r-selection and K-selection, with better abilities of exploring and exploiting, r/KPSO is expected to converge in higher precision than standard PSO [12,13].

5.2. **r/KPSO-RF.** r/KPSO-RF is a query optimization method of supervised study, which needs people to participate in the process. It mainly includes the methods named distance measurement and the machine learning. The methods based on distance measurement include query refinement method and reweighting method. Query refinement methods are simple to apply and can adjust query vector according to the positive and negative samples. For a group of relevance images D_R and irrelevance images D_N, the corresponding optimization query is defined as Equation (24):

$$Q' = \alpha Q + \beta \left(\frac{1}{|D_R|} \sum_{i \in D_R} D_i \right) - \gamma \left(\frac{1}{|D_N|} \sum_{i \in D_N} D_i \right) \tag{24}$$

where Q is the initial query, Q' is the optimized query, $|\cdot|$ is the size of set, α, β, γ are adjust parameters. Adjusting weightings of different feature dimensions, feature reweighting methods can optimize the retrieval results. In n dimension feature space, the weighted distance between given query vector $q = (q_1, q_2, \cdots, q_n)^T$ and feature vector $x = (x_{i1}, x_{i2}, \cdots, x_{in})^T$ is defined as Equation (25):

$$D(x_i, q, \omega) = \sum_{j=1}^{n} |(\omega_j \cdot \text{distance}(x_{ij}, q_j))| \tag{25}$$

In which ω is the weight to be adjusted during the query process. Then, we can obtain Equation (26) by generalizing the parameters of Equations (24) and (25).

$$\begin{aligned} S' &= \left\{ x_i \left| \text{distance} \left(\alpha \ \beta \ \gamma \right) \begin{pmatrix} S \\ D'_R \\ -D'_N \end{pmatrix} \cdot \omega, x_i \cdot \omega < \varepsilon \right. \right\}, \\ D'_R &= \frac{1}{|D_R|} \sum_{i \in D_R} D_i, \quad D'_N = \frac{1}{|D_N|} \sum_{i \in D_N} D_i \end{aligned} \tag{26}$$

where S' is the retrieval result after optimization and $\omega = (\omega_1, \omega_2, \cdots, \omega_n)^T$ is the weighting vector. Suppose the query and feedback results S, D'_R, D'_N are expressed with feature vectors $(C_{1S}, C_{2S}, \cdots, C_{nS})^T$, $(C_{1D'_R}, C_{2D'_R}, \cdots, C_{nD'_R})^T$, $(C_{1D'_N}, C_{2D'_N}, \cdots, C_{nD'_N})^T$, Equation (26) can be translated to Equation (27).

Then, we adopt r/KPSO to optimize the parameters according to S, D_R and D_N. The parameters' optimizing process is accomplished by the r/KPSO [14].

$$\begin{aligned} S' &= \left\{ x_i \left| \begin{pmatrix} \text{distance}'(\alpha C_{1S} + \beta C_{1D'_R} - \gamma C_{1D'_N}, x_{i1}) \\ \text{distance}'(\alpha C_{2S} + \beta C_{2D'_R} - \gamma C_{2D'_N}, x_{i2}) \\ \\ \text{distance}'(\alpha C_{nS} + \beta C_{nD'_R} - \gamma C_{nD'_N}, x_{in}) \end{pmatrix} \cdot \begin{pmatrix} \omega_1 \\ \omega_1 \\ \vdots \\ \omega_n \end{pmatrix} < \varepsilon \right. \right\} \\ &= \left\{ x_i \left| \sum_{j=1}^{n} \left(\omega_j \cdot \text{distance}'(\alpha C_{jS} + \beta C_{jD'_R} - \gamma C_{jD'_N}, x_{ij}) \right) < \varepsilon \right. \right\} \end{aligned} \tag{27}$$

6. **Experiments.** We use the same platform (software: Matlab7.1, hardware: Core 2 Q8200 CPU, 2.33GHz, 4.0GB memory) and adopt SIMPLIcity image database for the experiment in this paper (http://wang.ist.psu.edu/∼jwang/test1.tar). The images in database can divide into 10 categories, such as Africa, beaches, monument, busses, dinosaurs, elephants, flowers, horses, mountain, and cookie/food. Each class contains 100 images.

FIGURE 6. Diagrammatic sketch of ten classes

We randomly select one image in each class to constitute a diagrammatic sketch, as shown in Figure 6.

In the experiment, we divide the interest point's area into 6 annular parts. The number of interest point is set to 150. The color feature dimensions are set to 72. The parameters of r/KPSO are set according to Table 1. Query images are selected randomly in each class. Then, we calculate the precision of the retrieval result. The precision is defined as $P_T = n/T$. T represents the total number of output images in the retrieval result and n represents the number of correct images.

Figure 7 shows some retrieval results of first round by using our method. According to the interest of certain content, Users should mark the images with Yes or No. As shown in Figure 7, yes represents the positive sample, and no represents the negative sample. Figure 7(a) shows a retrieval result of Africa, which have 5 negative samples and the precision is 75%. Figure 7(b) shows a retrieval result of flower, which have 0 negative samples and the precision is 100%. Figure 7(c) shows a retrieval result of horses, which have 3 negative samples and the precision is 85%. Figure 7(d) shows a retrieval result for mountain, which have 3 negative samples and the precision is 85%.

Because the flower's precision is 100%, it does not need relevance feedback. We just need to do the subsequent procedures for Africa, horses and mountain by using four rounds r/KPSO-RF. There are negative samples in the final retrieval results, one in Africa, two in horses and two in mountain. The precisions promote to 90%, 95% and 90% respectively, as shown in Figure 8. All of the results are satisfied to our needs.

In order to evaluate the performance of the proposed method further, we compared the precision of different algorithms in [5,6]. Firstly, we randomly select 20 images for query in each class. Secondly, we retrieve these images and output the results. Finally, if the total number of output images is set to 10, 20 and 30, we calculate the average precision $\overline{P}_{10}$, $\overline{P}_{20}$ and $\overline{P}_{30}$ respectively, as shown in Table 2. We can see that the average precision of our method has increased 8.9 percent than the one of Ref. [5] and 8.0 percent than the one of Ref. [6].

Additionally, we compared the PVR performance with some popular methods, such as SVM-RF, PSORW-RF and ABRS-SVM, as shown in Figure 9. Because IDPSH algorithms detect the interest points more accurately and r/KPSO can converge in obviously higher

(a) Africa (b) Flowers

(c) Horses (d) Mountain

FIGURE 7. Retrieval results of first round

TABLE 2. Precision of different methods

Categories of images	$\overline{P}_{10}/\%$			$\overline{P}_{20}/\%$			$\overline{P}_{30}/\%$		
	Our	Ref. [5]	Ref. [6]	Our	Ref. [5]	Ref. [6]	Our	Ref. [5]	Ref. [6]
Africa	72.3	62.1	71.5	67.5	55.0	67.5	63.3	53.1	55.7
beaches	49.5	47.2	42.3	45.0	36.9	34.6	44.6	33.9	34.7
monument	78.1	69.5	68.0	74.5	58.6	59.4	72.3	55.4	56.1
busses	75.5	70.6	71.7	75.8	62.0	72.9	68.6	63.2	67.6
dinosaurs	98.2	91.0	94.2	94.6	89.3	91.0	93.8	84.7	86.2
elephants	72.0	63.4	54.0	58.1	45.7	43.2	47.4	39.3	37.3
flowers	93.6	88.3	81.0	88.6	78.4	72.3	92.0	68.4	64.3
horses	89.4	79.6	83.5	77.2	75.5	79.8	76.3	66.8	76.5
mountain	69.0	53.2	50.4	50.5	56.1	45.7	49.6	43.3	41.6
cookie	68.7	65.5	66.7	69.8	58.3	63.5	54.1	48.4	59.2
average	76.6	69.0	68.3	70.2	61.6	63.0	66.2	55.7	57.9

(a) Africa (b) Horses

(c) Mountain

FIGURE 8. Final results of feedback

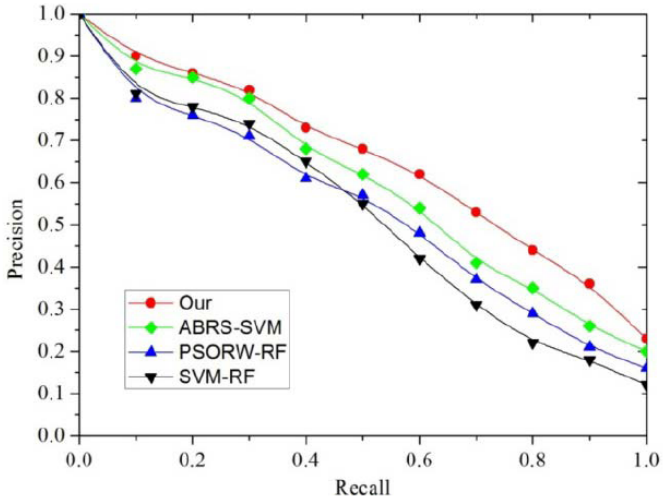

FIGURE 9. PVR curves of different methods

speed and precision than other PSO implementations, both the recall and precision of the method proposed are superior to the others.

7. **Conclusions and Future Work.** Through the analysis and compared with other methods, we found the proposed method have more advantages. The IPDSH algorithm can effectively eliminate the unstable interest points in the non-interest regions. Weighted feature of vector Pseudo-Zernike moments and annular color moment based on IPDSH are of a high retrieval speed and precision. Evolution searching by r/KPSO and user feedback can help to obtain a learning ability which improves the system's retrieval capabilities. There is something else, such as effective study, quick convergence in RF, overcomes ubiquitous problems, strong robustness and good retrieval effect.

However, image retrieval is a difficult problem. In the future, we will extend the proposed method to a large and complex database and try to improve the detection speed while guaranteeing accuracy.

Acknowledgment. This work was supported by the National Natural Science Foundation of China under Grants No. 61003196, No. 61201290, No. 61305040 and the Fundamental Research Funds for the Central Universities under Grants K50510040008, K505120400 11 and K5051304024.

REFERENCES

[1] C. H. Lee and M. F. Lin, Two active-dimension strategies for multi-query image retrieval, *ICIC Express Letters*, vol.5, no.8, pp.2675-2681, 2011.

[2] H. Y. Song, X. F. Li and P. J. Wang, Content- and semantic-based progressive multimodal image retrieval, *ICIC Express Letters*, vol.5, no.1, pp.201-206, 2011.

[3] L. N. Zhang, L. P. Wang and W. S. Lin, Semisupervised biased maximum margin analysis for interactive image retrieval, *IEEE Transactions on Image Processing*, vol.21, no.4, pp.2294-2308, 2012.

[4] Y. X. Li, B. Geng and D. C. Tao, Difficulty guided image retrieval using linear multiple feature embedding, *IEEE Transactions on Multimedia*, vol.14, no.6, pp.1618-1630, 2012.

[5] M. S. Chen, S. Y. Yang and Z. J. Zhao, Multi-points diverse density learning algorithm and its application in image retrieval, *Journal of Jilin University (Engineering and Technology Edition)*, vol.41, no.5, pp.1456-1460, 2011.

[6] C. H. Ma, Q. Dai and S. B. Liu, A hybrid PSO and active learning SVM model for relevance feedback in the content-based images retrieval, *Proc. of the International Conference on Computer Science and Service System*, Nanjing, China, pp.130-133, 2012.

[7] Y. T. Wang, Y. Q. Chen and J. Li, The Harris corner detection method based on three scale invariance spaces, *International Journal of Computer Science Issues*, vol.9, no.6, pp.18-22, 2012.

[8] X. B. Dai, T. L. Liu and H. Z. Shu, Pseudo-Zernike moment invariants to blur degradation and their use in image recognition, *Lecture Notes in Computer Science*, pp.90-97, 2013.

[9] T. Dobzhansky, Evolution in the tropics, *American Science*, vol.38, pp.209-221, 1950.

[10] R. H. MacArthus and E. O. Wilson, *The Theory of Island Biogeography*, Princeton Universtiy Press, Princetion, 1967.

[11] V. Z. Hadzi and N. Zlatanov, Outage rates and outage durations of opportunistic relaying systems, *IEEE Communications Letters*, vol.14, no.2, pp.148-150, 2010.

[12] Y. Y. Yan and B. L. Guo, Particle swarm optimization inspired by r- and K-selection in ecology, *Proc. of the IEEE Congress on Evolutionary Computation*, Hongkong, China, pp.1117-1123, 2008.

[13] B. Mattia and G. B. Francesco, A stochastic approach to image retrieval using relevance feedback and particle swarm optimization, *IEEE Transactions on Multimedia*, vol.12, no.4, pp.267-277, 2010.

[14] X. Zhang, B. L. Guo and G. Y. Zhang, An image retrieval method based on r/KPSO, *Proc. of the 2nd International Conference on Innovations in Bio-Inspired Computing and Applications*, Shenzhen, China, pp.69-72, 2011.